ORIGINAL ARTICLE

Smart Approaches of Nanosponge-loaded Gels of Ketoconazole for Topical Delivery

Ashima Ahuja, Meenakshi Bajpai

Department of Pharmacy, Institute of Pharmaceutical Research, GLA University, Mathura, Uttar Pradesh, India

Abstract

Aim: The present study was done to formulate ketoconazole (KET) nanosponges (NSs) using ethyl cellulose polymer using the solvent evaporation method. Materials and Methods: The prepared NSs were subjected to a drug-polymer incompatibility study using Fourier transform infrared analysis. In addition, formulations F1-F6 were evaluated for various parameters such as percentage yield, % entrapment efficiency (EE), % drug content, in vitro release study, and particle size determination using scanning electron microscopy analysis. **Results and Discussion:** KET-loaded EC nanosponges F6 optimized formulation showed superior % drug content, % yield, and EE, showing extended drug release of drug (84.48%) at the end of 240 minutes. Optimized formulation was loaded into HPMC gel and evaluated for pH, viscosity, extrudability, and % drug content. KET-NSs-loaded HPMC gel (GK5) showed optimal pH (4.24), good spreadibility (23.76 g.cm/sec), extrudability (96.14%), and viscosity (3567 cp). In vitro antifungal study revealed that KET-loaded NSs showed potent antifungal activity against C. albicans. GK5 formulation loaded with HPMC effectively targets fungal infection and is effective for topical delivery. **Conclusion:** The findings revealed that the nanosponges-loaded gel was effective for antifungal delivery.

Key words: *Candida albicans*, Fungal infection, *In vitro* release study, Ketoconazole, Nanosponges, Topical delivery

INTRODUCTION

Fungal infections, also called mycoses, affect millions of people worldwide. Fungus lives in soil, plants, skin, and household areas.[1] They are mainly found in moist areas and affect nails, toes, underarms, breasts, and genital areas. Fungal infection can penetrate deeper skin areas in persons with diabetes, resulting in rash, skin eruption, allergy, and irritation.[2] Fungal infections are diagnosed by scrapping skin surfaces and culturing fungal microbes. Dermatophytes such as *Candida albicans* are a natural micro-biome in the host body. It mainly stays in the gastrointestinal tract, vagina, and mouth areas. It leads to skin rashes, white spots, thrush, allergic reactions, and irritation.[3]

Nanotherapeutics have become popular in recent years due to their target-specific, productive, and patient-tailored delivery. Human skin is highly exposed to external environments of ultraviolet radiation, microbes, pH, and temperature, where nanoformulations offer advantages for topical delivery and improve patient compliance.[4-7]

Nanosponges (NSs) are microscopic solid nanoparticles that contain voids in their porous and spongy virus-like structure, made up of degradable polymers. They are a few nanometers in diameter with particle sizes of <1 µm. They can entrap lipophilic and hydrophilic drug molecules and improve the aqueous solubility of the dosage form. The tiny mesh-like structure and intercellular voids can effectively target antifungal, proteins, and anticancer drugs and produce 5 times more efficacy than conventional medication. NSs are novel drug formulations that can encapsulate nanoparticles and control the delivery of topical formulation by crosslinking with colloidal-based hyper crosslinked polymers. Nanoponges can deliver topical drugs by passive targeting that helps to reduce dose dumping, improves skin retention, reduces skin toxicity and irritation, and increases permeability, drug stability, and bioavailability, promoting patient compliance and health.[8,9]

Address for correspondence:
Ashima Ahuja, Department of Pharmacy, Institute of Pharmaceutical Research, GLA University, Mathura, 281406, Uttar Pradesh, India. E-mail: ashima.ahuja@gla.ac.in

Received: 19-01-2025
Revised: 19-03-2025
Accepted: 29-03-2025

Scientists have formulated nystatin chitosan and alginate microspheres using emulsification and gelation methods to manage fungal infection. The prepared hydrogel effectively worked against *C. albicans* in oral mucosa, promoting buccal vehiculation of nystatin.[10] Ketoconazole (KET) is a potent antifungal drug that prevents ergosterol synthesis, increases membrane fluidity, and prevents fungal growth. It is a fungistatic agent that inhibits fungal cell growth and prevents fungus from spreading throughout the body. It effectively manages fungal infections such as thrush, allergy, mycosis, ringworm, and vulvovaginal infection. It is a potent inhibitor of the squalene epoxidase enzyme and becomes deficient in ergosterol, an essential component of fungal cell membranes.[11,12]

Fungal infections that are sometimes become serious and result in death. Dermal infections are the prevailing cause of socioeconomic burden that affects humankind worldwide. Although it is considerably non-fatal, it sometimes becomes lethal due to negligence, improper management, or treatment. Several scientific studies highlighted the importance of advanced herbal, synthetic formulations for managing dermatological infections using conventional and alternative therapies. Herbal remedies and conventional medications are widely explored for treating pathological skin disorders such as acne, athlete's foot, fungal infection, eczema, psoriasis, albinism, vitiligo, and skin pigmentation. Results of scientific data suggested that conventional formulations have proven therapeutic benefits against skin ailments. Herbal bioactive obtained from various botanicals is also helpful in the management of dermatological disorders. Homemade remedies are used for curing various skin ailments and promote treatment for herbal formulations with low toxicity and reduced side effects.[13-19]

Pathophysiology of fungal Infection

Aspergillosis is a serious invasive infection that mainly spreads through inhalation of spores or by invading damaged skin. It also infects patients with a previous history of lung infections, HIV/AIDS, and immunocompromised patients.

Major risk

- Receiving a dose for more than 7 days causes neutropenia
- Requires frequent dosing as corticosteroid therapy
- May results in heredity disorders
- Problems in organ transplantation.[20-22]

MATERIALS AND METHODS

KET (API) was obtained from Chemland Pvt. Ltd., a Gujarat gift sample. All the other polymers, ethyl cellulose (EC), polyvinyl alcohol (PVA), PG, and reagents were of analytical grade and used to formulate NSs and topical gel, as depicted in Table 1.

METHOD OF PREPARATION FOR KET-NSS

Solvent evaporation method

KET-NSs (F1-F6) were prepared using the solvent evaporation method by dissolving EC polymer in the organic solvent phase (10 mL dichloromethane [DCM]) as an internal phase. Further, 1% w/v PVA was added to distilled water 100 mL as an external phase and stirred on a magnetic stirrer at 1000–1500 rpm for 2–3 h. The internal phase was dropwise poured using a 22 gauge microneedle into the external phase containing PVA, and stirring was continued further to form NSs. The resultant preparation was kept undisturbed for 24 h. The resulting solution was filtered and dried at room temperature overnight, as explained in Table 2, Figures 1 and 2. The dried NSs were stored and evaluated for the following parameters.[23-25]

NANOSPONGES: CHARACTERIZATION PARAMETERS (KET-NSS)

Drug polymer incompatibility

Fourier transform infrared (FTIR) analysis

Finely powdered KET (pure drug), polymer EC, PVA, physical mixture (PM), and KET-loaded NSs were analyzed by an FTIR spectrophotometer (Shimadzu, Kyoto, Japan) to determine drug-excipient incompatibility.[26-29]

Particle size

Scanning electron microscopy (SEM)

An SEM (JEOL JSM-1010-LA) operating at 20 kV was examined for surface morphology at Jamia Hamdard, New Delhi. A photograph was recorded at ×100, ×500, and ×1000 magnification.[30-34]

% age production yield

Drug-loaded NSs were weighed after drying and dried NSs' % age production yield was determined using the formula as follows:[30-34]

% yield: wt of dried NSs/mass of drug and polymer (total mass) + drug × 100.

Table 1: Formulation ingredients of nanosponges and topical gel

S. No.	Materials	Company Manufacturers	Category and Applications
1	Ketoconazole (KET)	Chemland Pvt. Ltd.	Antifungal, topically used in nanoparticles, nanosponge microspheres, and antifungal gel formulation
2	Ethylcellulose (EC)	HiMedia Laboratories Pvt. Ltd.	Nanopsonge formulation polymer
3	Polyvinyl Alcohol (PVA)	HiMedia Laboratories Pvt. Ltd	Nanopsonge formulation polymer
4	Dichloromethane (DCM)	SDL	Nanopsonge formulation Solvent
5	Carbopol-934 (CP)	SDL	Topical gel formulation gelling agent
6	Hydroxypropyl methylcellulose (HPMC)	SDL	Topical gel formulation gelling agent
7	Triethanolamine (TEA)	LobiaChemie Pvt. Ltd. Mumbai	Topical gel formulation buffer
8	Methylparaben (MP)	HiMedia Laboratories Pvt. Ltd	Topical gel formulation preservatives
9	Alcohol, methanol	Changshu Hangsheng fine chemical Co Ltd	Topical gel formulation Diluent and penetration enhancer

Table 2: Formulation of KET-EC nanosponges (F1-F6) and selection of optimized formulation

Formulation codes	KET (Drug mg)	EC (g)	Dichloromethane (mL)	PVA (%)
F1	150	0.5	10	1
F2	150	1	10	1
F3	150	1.5	10	1
F4	150	2	10	1
F5	150	2.5	10	1
F6	150	3	10	1

EC: Ethylcellulose, KET: Ketoconazole, PVA: Polyvinyl alcohol

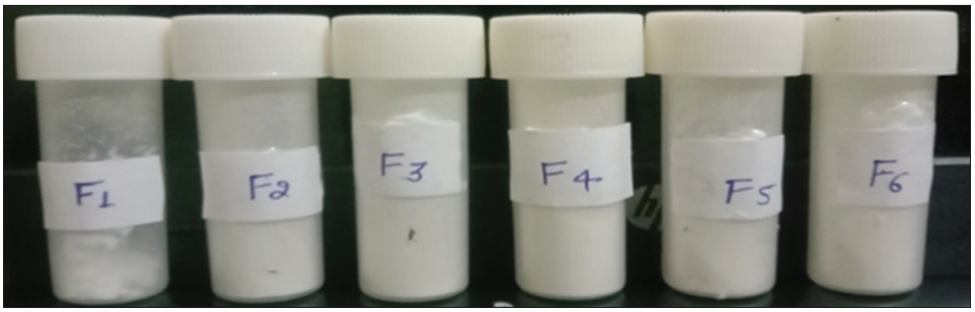

Figure 1: Different nanosponge formulation (Ketoconazole-Nanosponges F1-F6)

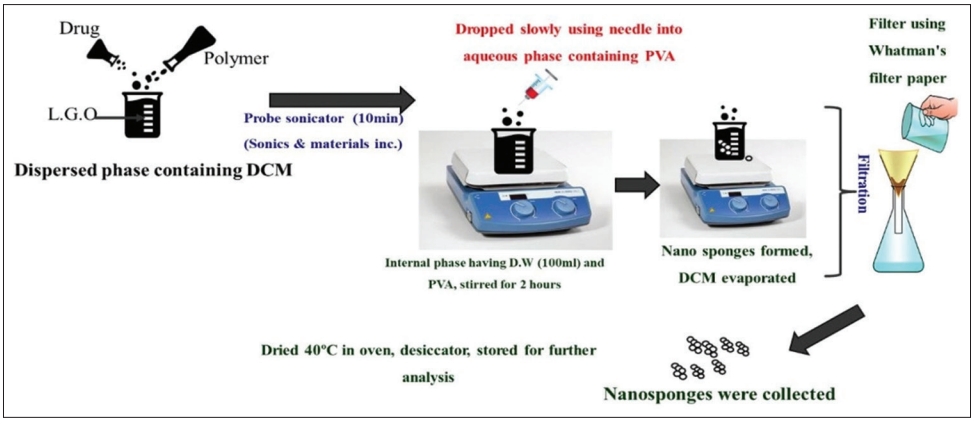

Figure 2: Emulsion solvent evaporation method

Table 3: Topical gel composition (GK1-GK6)

S. No.	Formulation (w/w%)	GK1	GK2	GK3	GK4	GK5	GK6
1.	NSs (mg)	200	200	200	200	200	200
2.	HPMC (g)	-	-	-	1	2	3
3.	CP (g)	1	2	3	-	-	-
4.	Glycerin (mL)	8	8	8	8	8	8
5.	Methanol (mL)	6	8	8	8	8	8
6.	TEA (mL)	0.2	0.2	0.2	0.2	0.2	0.2
7.	MP	0.01	0.01	0.01	0.01	0.01	0.01
8.	DW (mL)	50	50	50	50	50	50

NSs: Nanosponges, HPMC: Hydroxypropylmethylcellulose, CP: Carbopol-934, TEA: Triethanolamine, MP: Methyl paraben, DW: Distilled water

Table 4: Calibration curve of ketoconazole in phosphate-buffered saline (6.8) or phosphate buffer

S. No.	Concentration (g/mL)	Absorbance 278 nm (Ketoconazole)
1	10	0.658
2	20	1.232
3	30	1.878
4	40	2.546
5	50	3.098

Table 5: FTIR spectra peaks of ketoconazole

Groups	IR peaks (Observed)	IR peaks (Reported)
CH_2	1437.47 cm^{-1}	1450.43 cm^{-1}
C-H	2975.40 cm^{-1}	3000–2850 cm^{-1}
C=O	1667.12 cm^{-1}	1680–1630 cm^{-1}
C-N	1375.75 cm^{-1}, 1053.52 cm^{-1}	1350–1000 cm^{-1}

FTIR: Fourier transform infrared

Table 6: FTIR spectra peaks of EC

Groups	IR peaks (Observed)	IR peaks (Reported)
C-H	2975.40 cm^{-1}	2960–2850 cm^{-1}
C=O	1810.65 cm^{-1}	1820–1665 cm^{-1}
O-H	3371.55 cm^{-1}	3650–3200 cm^{-1}

FTIR: Fourier transform infrared, EC: Ethyl cellulose

Table 7: FTIR spectra peaks of PVA

Groups	IR peaks (Observed)	IR peaks (Reported)
CH_2	2903.64 cm^{-1}	2941.43 cm^{-1}
O-H	3688.75 cm^{-1}	3000–3700 cm^{-1}

FTIR: Fourier transform infrared, PVA: Polyvinyl alcohol

Percentage entrapment efficiency (EE)

Prepared KET-NSs were dried, weighed (100 mg), dissolved in 10 mL methanol, and ultracentrifuged at 15,000 rpm. The resultant mixture was filtered, and a supernatant layer containing free drug was collected, diluted, and analyzed spectrophotometrically (Shimadzu) at 278 nm. The experiment was repeated in triplicates to obtain % EE at 4.5 pH phosphate-buffered saline (PBS). The percentage of EE was calculated using the following formula:

% EE= Total drug-free amount of drug/total drug × 100.

TOPICAL GEL PREPARATION

Prepared and dried KET-NSs (200 mg) each were loaded with gelling agents such as sodium alginate and hydroxypropylmethylcellulose (HPMC) to form 50 g topical gels (GK1-GK6). It is done by soaking the gelling agent overnight in 250 mL of distilled water to form a gel base. Polymeric gel base was then neutralized with triethanolamine. Methylparaben (preservative) solution was dissolved in water and slowly incorporated to create a homogenous gel. Glycerin acts as a moistening agent, and methanol as a penetration enhancer was also used during the formulation of the gel base[35-37] depicted in Table 3.

EVALUATION OF TOPICAL GEL[38-47]

Physical appearance

All the prepared gels were visually examined for transparency, odor, and color [Table 8].

pH determination

The pH of the topical gels was measured using a digital pH meter, represented in [Table 8].

Table 8: FTIR spectra peaks of carbopol

Groups	IR peaks (Observed)	IR peaks (Reported)
C-H	703.02 cm^{-1}	753.15 cm^{-1}
C=C	3015.67 cm^{-1}	3041.78 cm^{-1}
C=N	1171.73 cm^{-1}	1741–1000.47 cm^{-1}
C-N	3688.75 cm^{-1}	3000–3700 cm^{-1}

FTIR: Fourier transform infrared

Table 9: FTIR spectra peaks of HPMC

Groups	IR peaks (Observed)	IR peaks (Reported)
C-H	2957.46 cm^{-1}	2927 cm^{-1} stretching of methyl and propyl group
C-O	1662.81 cm^{-1}	1691 cm^{-1} and 1610 cm^{-1}
C-O-C	1044.19 cm^{-1} and 943 cm^{-1}	1057 cm^{-1} and 946 cm^{-1} (due to pyranose ring and C-O-C stretching

FTIR: Fourier transform infrared, HPMC: Hydroxypropylmethylcellulose

Table 10: FTIR spectra peaks of KET+physical mixture of polymers

Groups	IR peaks (Observed)	IR peaks (Reported)
C-H	702.00 cm^{-1}	753.15 cm^{-1}
C=C	3005.10 cm^{-1}	3041.78 cm^{-1}
C=N	1105.00 cm^{-1}	1741–1000.47 cm^{-1}
C-N	3687.00 cm^{-1}	3000–3700 cm^{-1}

FTIR: Fourier transform infrared, KET: Ketoconazole

Spreadability determination

Prepared gels were placed between two slides; one end was tied with thread, and weight was placed. The time taken by the two slides to slip determines the spreadability, calculated using the formula:[36]

Spreadability (S) = W × L/T, where W denotes weight applied on the upper slide, L represents the length of the upper slide, and T indicates the time both sides take to separate.

Viscosity determination

The viscosity of the prepared topical gel was determined using a Brookfield LV viscometer [Table 8].

Extrudability determination

Prepared topical gels were loaded in the collapsible tube and allowed to excrude out. The extrudability was determined in terms of weights/gram required to extrude a 0.5 cm ribbon of gel in 10 s.

% Drug content

About 100 mg of each gel formulation was added to a 100 mL volumetric flask containing phosphate buffer (100 mL) pH 6.8, stirred for 30 min, and allowed to stand for 24 h. 0.5 mL of the above solution was pipetted out, diluted to 10 mL with phosphate buffer pH 6.8, and filtered through a membrane filter 0.45 μm, analyzed at 278 nm.

% In vitro drug release (dialysis bag method)

Nanosponge-loaded topical gel equivalent to 10 mg KET-NSs was kept in a dialysis bag subjected to the diffusion of a drug for 6 h [Figure 3]. At predetermined time intervals of 30, 60, 90, 120, 150, 180, 210, 240, 270, 300, 330, and 360 min, 5 mL samples of aliquots were pipetted out and replaced with fresh samples of methanolic phosphate buffer pH 6.8. The samples were then analyzed using the UV-visible spectrophotometer (278 nm) to determine the drug concentration released [Figures 3-5 and Table 4].

In vitro antifungal activity (disk diffusion method) against *C. albicans*

The antifungal activity of optimized GK5 gel, pure drug, KET-NSs, and the marketed formulation was determined using the disk diffusion method having a 6 mm diameter against *C. albicans*. A 6 mm disk was cut, dipped in the fungal solution, placed over solidified agar media in different Petri plates, and incubated at 32°C in a BOD incubator. Growth was observed after 24 h, and a zone of inhibition (ZOI) was measured.[48-55]

RESULTS AND DISCUSSION

FTIR studies

The FTIR study of KET, EC, PVA, and PM and drug-loaded NSs showed fundamental peaks; results suggested no incompatibility or interaction between drug and polymers was observed [Figures 6-12] and [Table 5-10].

Interpretation

No change in IR spectra was observed with a blend of polymer and drug.

Morphological study: SEM

The morphology of the optimized NSs F6 was determined by SEM analysis that showed formulated NSs were spherical and spongy [Figure 13].

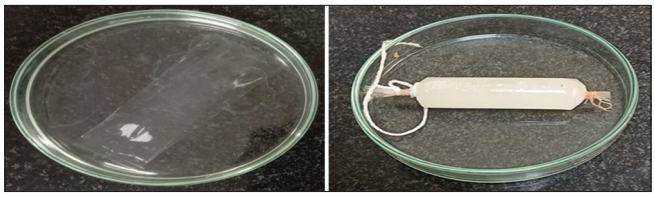

Figure 3: Prepared of cylindrical dialysis membrane bag (nanosponges suspended in buffer)

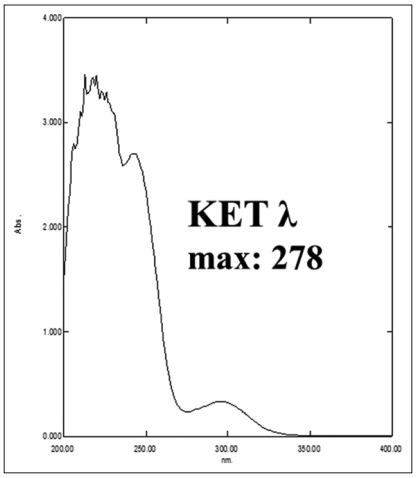

Figure 4: Absorption maxima of ketoconazole

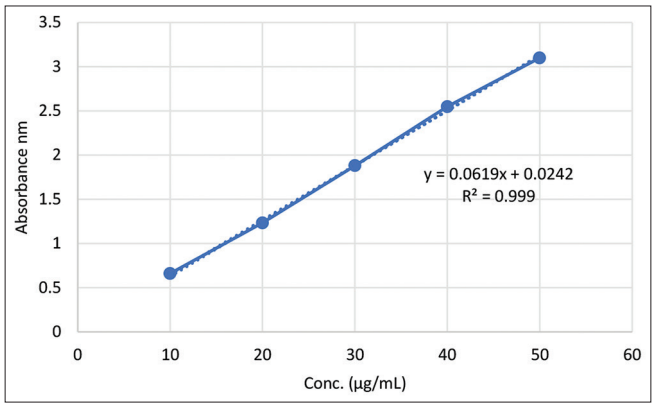

Figure 5: Calibration graph of ketoconazole (278 nm)

% yield and % EE

F1–F6 NSs were prepared. The resultant F6 formulation showed maximum % age production yield and % EE as depicted in Table 11 and Figure 14.

The production yield of all batches ranged from 36.43 ± 0.51 to 82.38 ± 0.58, suggesting that the drug: polymer ratio, along with PVA, significantly affects the % yield. In the case of F1 (36.43 ± 0.51), the % yield was low compared to F6 (82.38 ± 0.58), suggesting an increased drug: polymer ratio and an increase in % yield were observed, suggesting diffusion of DCM from the concentrated polymer solution to the aqueous phase. Furthermore, it provides additional time for droplet formation and increasing % yield.

% *In vitro* drug release

In vitro drug release was carried out in the Franz diffusion cell. Formulation F6 showed the best results at pH 6.8. The *in vitro* drug release was observed to decline in the range of 84.48–15.08% for formulations F3-F6, concerning the drug-to-polymer ratio. This suggested that with an increase in drug: polymer ratio for each NSs for encapsulating drug, the amount of polymer available was more, causing thickening in the polymer matrix wall. This further extends the diffusion path, causing reduced drug release. Initially, burst release was observed in F2-F5 formulations, suggesting that the encapsulated drug exists on the nearer surface or the exterior part of the NSs. Further, it was observed that the drug release was decreased with changes in the drug: polymer ratio in formulations (F1-F6) due to the complete swelling of the polymer matrix, and the time required for swelling becomes directly proportional to the polymer amount. Comparative drug release is observed and represented in Table 12 and Figure 15.

Marketed formulation of KET-NSs (pure drug)

The observed drug release study is mentioned in Table 12 and Figure 15, showing 86.34 at the end of 120 min for marketed preparation. It is because the drug got exhausted from the marketed gel compared to the encapsulated NSs present in formulation F6, showing slow drug release (84.48%) at the end of 240 min. This suggested that sustained effect was observed, and prepared formulations were targeted to reduce side effects of conventional medication such as irritation and hypersensitivity and improve drug release.

Evaluation of NSs-loaded topical gel

Physical appearance

The prepared formulations GK5 containing HPMC (2 g) and GK2 containing carbopol-934 (2 g) showed a light transparent, gray appearance, and absence of lumps [Table 13].

pH determination

pH was found to be 4.24 and 4.36 for formulations GK5 and GK2, suggesting formulations were effective for topical delivery, respectively, as shown in [Table 13].

Spreadability of loaded gels

The prepared formulations GK5 containing HPMC (2 g) and GK2 containing CP-934 (2 g) showed 23.76 and 20.04 (g.cm/s) spreadability [Table 13].

Viscosity

The viscosity of GK5 (2 g) and GK2 (2 g) gel formulations was found to be 3567 cp and 3257 cps, respectively [Table 13].

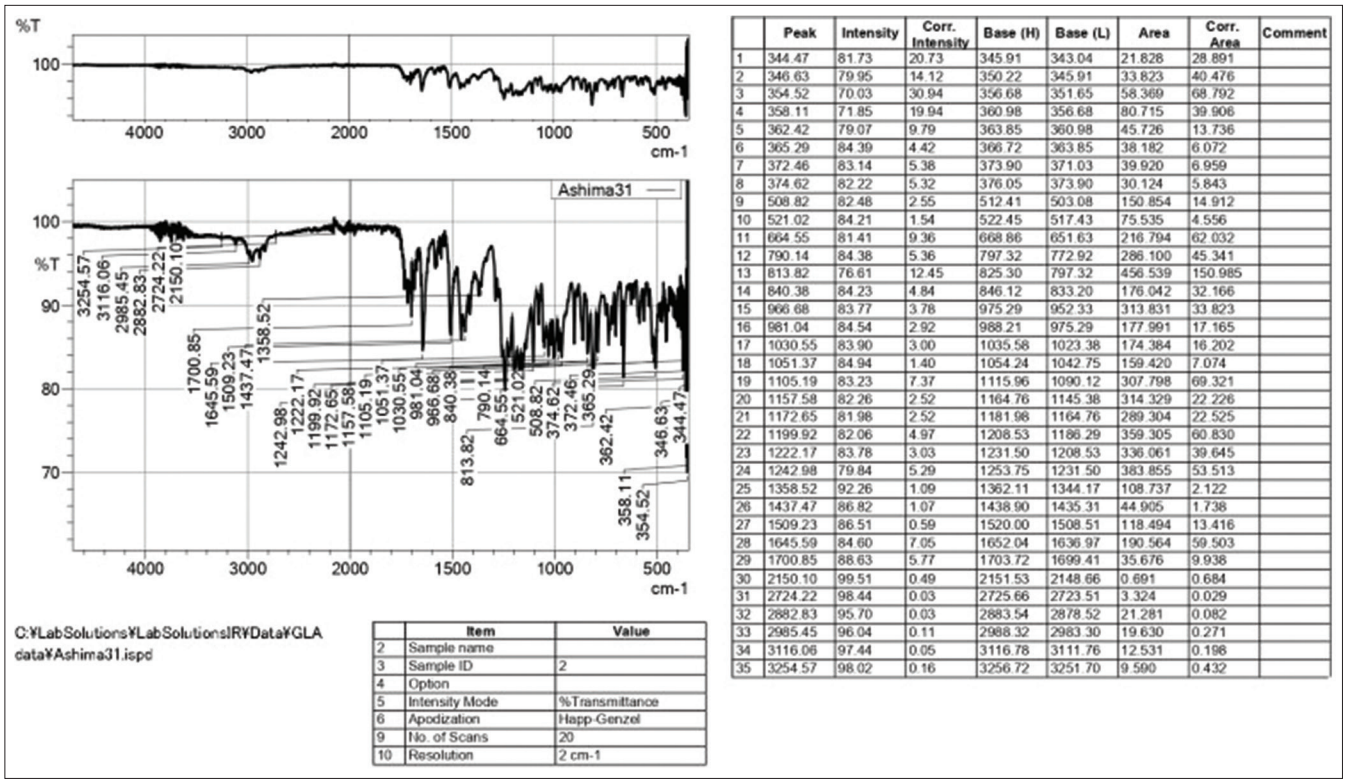

	Item	Value
2	Sample name	
3	Sample ID	2
4	Option	
5	Intensity Mode	%Transmittance
6	Apodization	Happ-Genzel
9	No. of Scans	20
10	Resolution	2 cm-1

	Peak	Intensity	Corr. Intensity	Base (H)	Base (L)	Area	Corr. Area	Comment
1	344.47	81.73	20.73	345.91	343.04	21.828	28.891	
2	346.63	79.95	14.12	350.22	345.91	33.823	40.476	
3	354.52	70.03	30.94	356.68	351.65	58.369	68.792	
4	358.11	71.85	19.94	360.98	356.68	80.715	39.906	
5	362.42	79.07	9.79	363.85	360.98	45.726	13.736	
6	365.29	84.39	4.42	366.72	363.85	38.182	6.072	
7	372.46	83.14	5.38	373.90	371.03	39.920	6.959	
8	374.62	82.22	5.32	376.05	373.90	30.124	5.843	
9	508.82	82.48	2.55	512.41	503.08	150.854	14.912	
10	521.02	84.21	1.54	522.45	517.43	75.535	4.556	
11	664.55	81.41	9.36	668.86	651.63	216.794	62.032	
12	790.14	84.38	5.36	797.32	772.92	286.100	45.341	
13	813.82	76.61	12.45	825.30	797.32	456.539	150.985	
14	840.38	84.23	4.84	846.12	833.20	176.042	32.166	
15	966.68	83.77	3.78	975.29	952.33	313.831	33.823	
16	981.04	84.54	2.92	988.21	975.29	177.991	17.165	
17	1030.55	83.90	3.00	1035.58	1023.38	174.384	16.202	
18	1051.37	84.94	1.40	1054.24	1042.75	159.420	7.074	
19	1105.19	83.23	7.37	1115.96	1090.12	307.798	69.321	
20	1157.58	82.26	2.52	1164.76	1145.38	314.329	22.226	
21	1172.65	81.98	2.52	1181.98	1164.76	289.304	22.525	
22	1199.92	82.06	4.97	1208.53	1186.29	359.305	60.830	
23	1222.17	83.78	3.03	1231.50	1208.53	336.061	39.645	
24	1242.98	79.84	5.29	1253.75	1231.50	383.855	53.513	
25	1358.52	92.26	1.09	1362.11	1344.17	108.737	2.122	
26	1437.47	86.82	1.07	1438.90	1435.31	44.905	1.738	
27	1509.23	86.51	0.59	1520.00	1508.51	118.494	13.416	
28	1645.59	84.60	7.05	1652.04	1636.97	190.564	59.503	
29	1700.85	88.63	5.77	1703.72	1699.41	35.676	9.938	
30	2150.10	99.51	0.49	2151.53	2148.66	0.691	0.684	
31	2724.22	98.44	0.03	2725.66	2723.51	3.324	0.029	
32	2882.83	95.70	0.03	2883.54	2878.52	21.281	0.082	
33	2985.45	96.04	0.11	2988.32	2983.30	19.630	0.271	
34	3116.06	97.44	0.05	3116.78	3111.76	12.531	0.198	
35	3254.57	98.02	0.16	3256.72	3251.70	9.590	0.432	

Figure 6: Fourier transform infrared spectra of ketoconazole

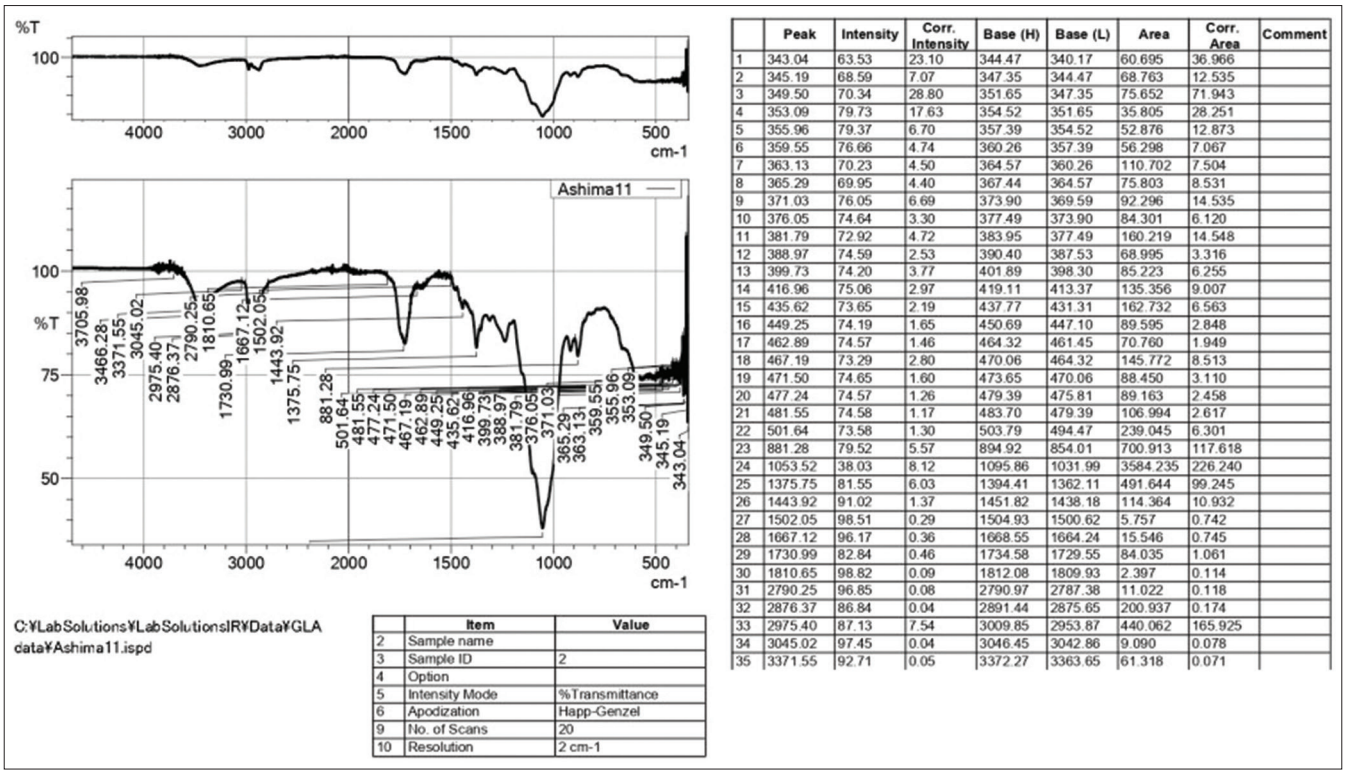

	Item	Value
2	Sample name	
3	Sample ID	2
4	Option	
5	Intensity Mode	%Transmittance
6	Apodization	Happ-Genzel
9	No. of Scans	20
10	Resolution	2 cm-1

	Peak	Intensity	Corr. Intensity	Base (H)	Base (L)	Area	Corr. Area	Comment
1	343.04	63.53	23.10	344.47	340.17	60.695	36.966	
2	345.19	68.59	7.07	347.35	344.47	68.763	12.535	
3	349.50	70.34	28.80	351.65	347.35	75.652	71.943	
4	353.09	79.73	17.63	354.52	351.65	35.805	28.251	
5	355.96	79.37	6.70	357.39	354.52	52.876	12.873	
6	359.55	76.66	4.74	360.26	357.39	56.298	7.067	
7	363.13	70.23	4.50	364.57	360.26	110.702	7.504	
8	365.29	69.95	4.40	367.44	364.57	75.803	8.531	
9	371.03	76.05	6.69	373.90	369.59	92.296	14.535	
10	376.05	74.64	3.30	377.49	373.90	84.301	6.120	
11	381.79	72.92	4.72	383.95	377.49	160.219	14.548	
12	388.97	74.59	2.53	390.40	387.53	68.995	3.316	
13	399.73	74.20	3.77	401.89	398.30	85.223	6.255	
14	416.96	75.06	2.97	419.11	413.37	135.356	9.007	
15	435.62	73.65	2.19	437.77	431.31	162.732	6.563	
16	449.25	74.19	1.65	450.69	447.10	89.595	2.848	
17	462.89	74.57	1.46	464.32	461.45	70.760	1.949	
18	467.19	73.29	2.80	470.06	464.32	145.772	8.513	
19	471.50	74.65	1.60	473.65	470.06	88.450	3.110	
20	477.24	74.57	1.26	479.39	475.81	89.163	2.458	
21	481.55	74.58	1.17	483.70	479.39	106.994	2.617	
22	501.64	73.58	1.30	503.79	494.47	239.045	6.301	
23	881.28	79.52	5.57	894.92	854.01	700.913	117.618	
24	1053.52	38.03	8.12	1095.86	1031.99	3584.235	226.240	
25	1375.75	81.55	6.03	1394.41	1362.11	491.644	99.245	
26	1443.92	91.02	1.37	1451.82	1438.18	114.364	10.932	
27	1502.05	98.51	0.29	1504.93	1500.62	5.757	0.742	
28	1667.12	96.17	0.36	1668.55	1664.24	15.546	0.745	
29	1730.99	82.84	0.46	1734.58	1729.55	84.035	1.061	
30	1810.65	98.82	0.09	1812.08	1809.93	2.397	0.114	
31	2790.25	96.85	0.08	2790.97	2787.38	11.022	0.118	
32	2876.37	86.84	0.04	2891.44	2875.65	200.937	0.174	
33	2975.40	87.13	7.54	3009.85	2953.87	440.062	165.925	
34	3045.02	97.45	0.04	3046.45	3042.86	9.090	0.078	
35	3371.55	92.71	0.05	3372.27	3363.65	61.318	0.071	

Figure 7: Fourier transform infrared spectra of ethyl cellulose

Extrudability

Extrudability was found to be GK5 (2 g) and GK2 (2 g) gel formulations were found at 96.14% and 85.24%, respectively, as compared to pure unentrapped drug-containing gel (100%). This suggested prepared formulation showed better extrudability [Table 13].

Table 11: Comparative data of yield (%) and % entrapment efficiency (KET-NSs)

Formulation codes	% yield±SD	% EE±SD
F1	36.43±0.51	44.56±0.55
F2	48.25±0.83	51.25±0.45
F3	66.32±0.44	67.12±0.55
F4	77.28±0.13	62.19±0.74
F5	65.71±0.55	72.38±0.80
F6	82.38±0.58	84.38±0.11

*SD: Standard deviation, *n*=3, KET: Ketoconazole, NS: Nanosponges

Table 12: % *In vitro* drug release: KET-NSs, pure drug at PO4 buffer (pH 6.8)

Time (min)	0	15	30	60	90	120	150	180	210	240	270	300	330	360
F1	Spherical Nanosponges were not formed													
F2														
F3	0	15.02	19.24	25.47	35.41	41.17	47.12	50.04	47.14	44.87	45.74	39.14	33.14	27.56
F4	0	17.21	23.45	32.12	40.19	47.25	57.1	63.14	67.24	63.14	62.12	58.41	55.21	47.38
F5	0	19.24	28.12	38.14	48.25	57.24	65.71	71.65	74.85	75.12	72.14	70.65	68.21	63.98
F6	0	21.25	34.25	47.65	55.24	66.21	71.35	75.21	78.84	84.48	77.14	75.21	70.65	68.56
Pure drug (MF)	0	27.12	53.98	77.54	86.34	88.24	68.45	55.14	37.12	21.01	14.25	10.27	7.98	6.12

KET: Ketoconazole, NS: Nanosponges

Table 13: Topical gel evaluation parameters (formulations GK2 and GK5)

S. No.	Parameters	Gelling agents (2 g each)	
		GK5 (HPMC)	GK2 (CP-934)
1.	pH	4.24	4.36
2.	Physical Appearance	Transparent (light), absence of lumps	Grayish, absence of lumps
3.	Spreadability	23.76 g.cm/sec	20.04 g.cm/sec
4.	Viscosity	3567 centipoises (cp)	3257 centipoises (cp)
5.	Extrudability	96.14%	85.24%

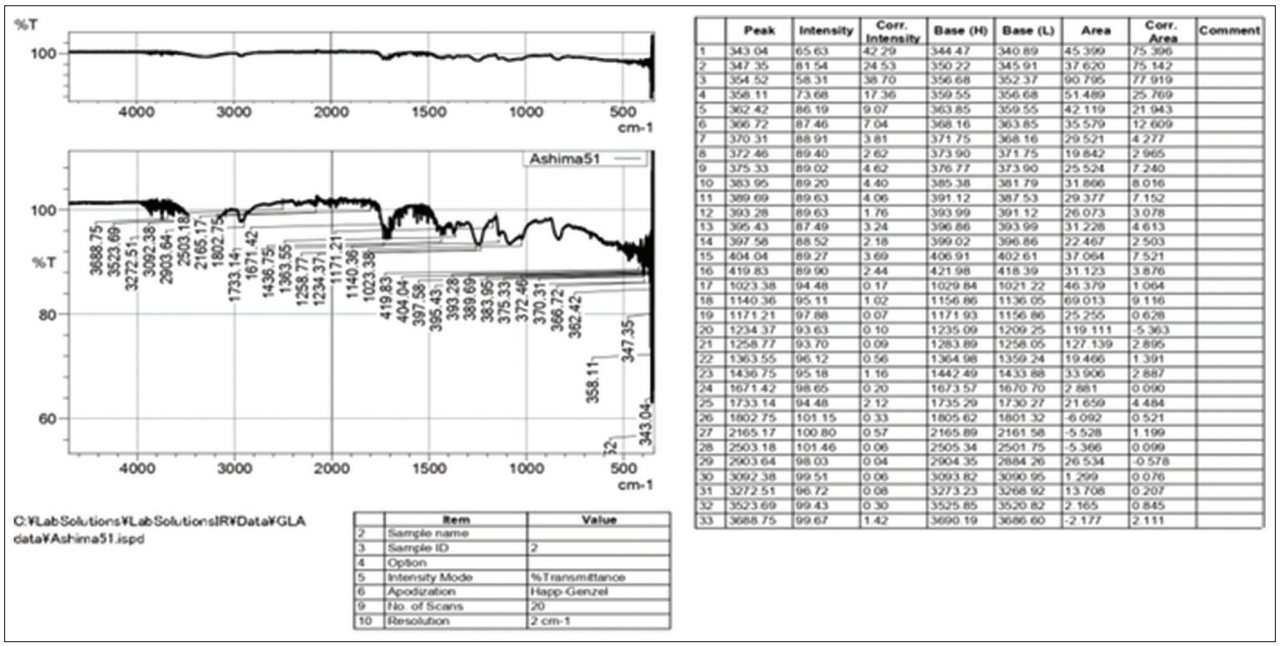

Figure 8: Fourier transform infrared spectra of polyvinyl alcohol

% In vitro drug release of KET-loaded gel

The *in vitro* drug release of KET-NSs-loaded gels for formulations GK2 and GK5 at pH 6.8 and 5.6 phosphate buffer, respectively, is determined, represented in Table 14, Figures 16 and 17.

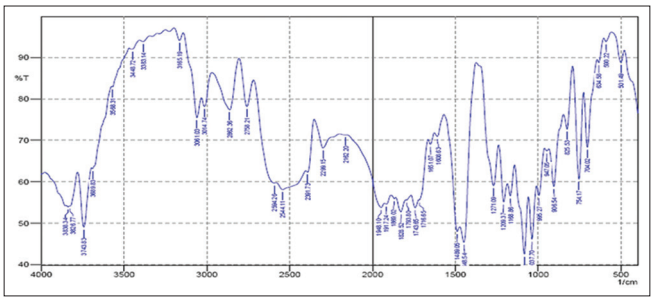

Figure 9: Fourier transform infrared spectra of carbopol

In vitro antifungal activity against *C. albicans* (optimized gel GK5)

Results of the *in vitro* antifungal study revealed that KET-loaded NSs showed potent antifungal activity against *C. albicans*; they can inhibit fungus growth. Furthermore, the *in vitro* disk diffusion method was used to estimate zone diameters (ZOI). Results suggested that C. albicans was highly susceptible to antifungal drug (KET) and showed ZOI surrounding the pure drug. This confirmed the susceptibility of the drug toward the virulent fungal strain, thus attributing

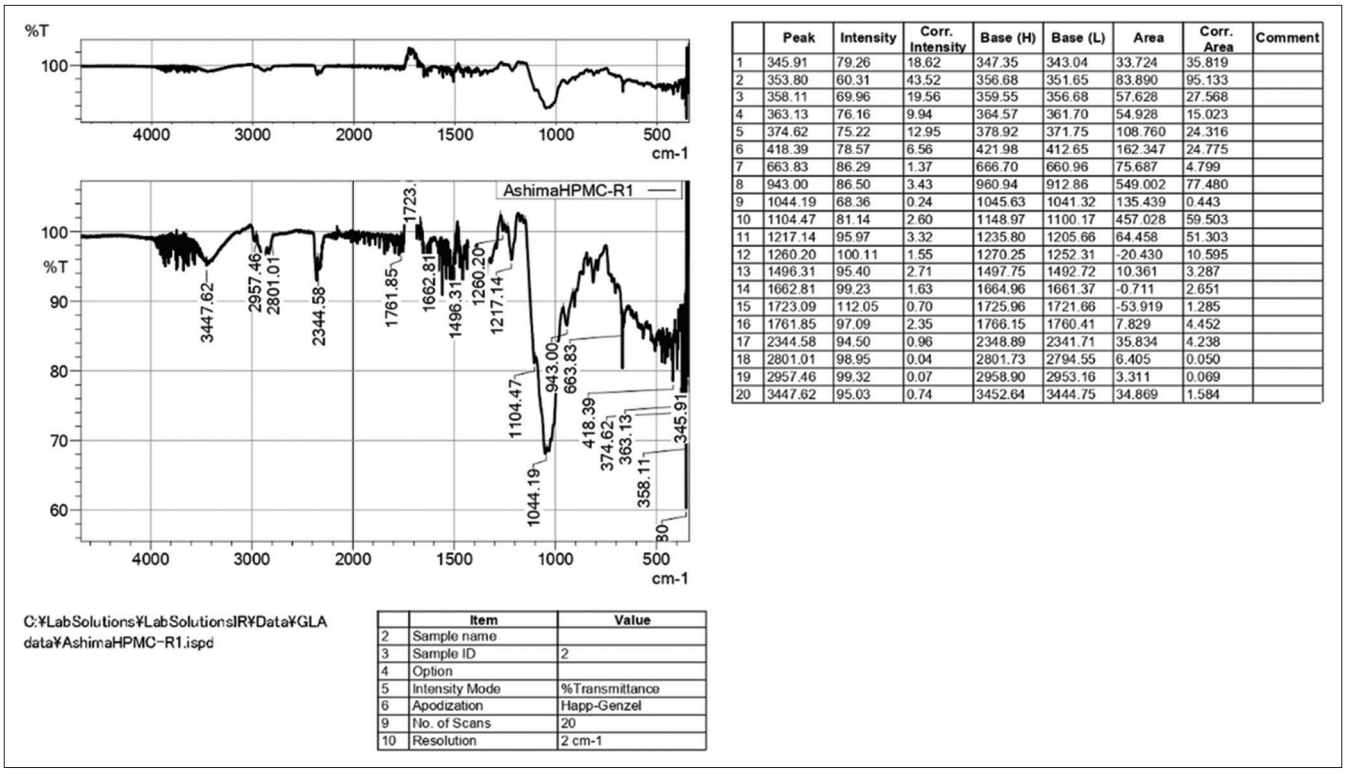

	Peak	Intensity	Corr. Intensity	Base (H)	Base (L)	Area	Corr. Area	Comment
1	345.91	79.26	18.62	347.35	343.04	33.724	35.819	
2	353.80	60.31	43.52	356.68	351.65	83.890	95.133	
3	358.11	69.96	19.56	359.55	356.68	57.628	27.568	
4	363.13	76.16	9.94	364.57	361.70	54.928	15.023	
5	374.62	75.22	12.95	378.92	371.75	108.760	24.316	
6	418.39	78.57	6.56	421.98	412.65	162.347	24.775	
7	663.83	86.29	1.37	666.70	660.96	75.687	4.799	
8	943.00	86.50	3.43	960.94	912.86	549.002	77.480	
9	1044.19	68.36	0.24	1045.63	1041.32	135.439	0.443	
10	1104.47	81.14	2.60	1148.97	1100.17	457.028	59.503	
11	1217.14	95.97	3.32	1235.80	1205.66	64.458	51.303	
12	1260.20	100.11	1.55	1270.25	1252.31	-20.430	10.595	
13	1496.31	95.40	2.71	1497.75	1492.72	10.361	3.287	
14	1662.81	99.23	1.63	1664.96	1661.37	-0.711	2.651	
15	1723.09	112.05	0.70	1725.96	1721.66	-53.919	1.285	
16	1761.85	97.09	2.35	1766.15	1760.41	7.829	4.452	
17	2344.58	94.50	0.96	2348.89	2341.71	35.834	4.238	
18	2801.01	98.95	0.04	2801.73	2794.55	6.405	0.050	
19	2957.46	99.32	0.07	2958.90	2953.16	3.311	0.069	
20	3447.62	95.03	0.74	3452.64	3444.75	34.869	1.584	

	Item	Value
2	Sample name	
3	Sample ID	2
4	Option	
5	Intensity Mode	%Transmittance
6	Apodization	Happ-Genzel
9	No. of Scans	20
10	Resolution	2 cm-1

Figure 10: Fourier transform infrared spectra of hydroxypropylmethylcellulose

Table 14: *In vitro* drug release studies of nanosponge-loaded gel and pure drug at phosphate buffer (pH 6.8 and pH 5.6)

pH 6.8 (Phosphate buffer)														
Time (min)	0	15	30	60	90	120	150	180	210	240	270	300	330	360
GK2	0	15.24	23.46	33.14	47.12	51.47	62.18	71.89	76.24	81.14	77.14	73.87	70.02	68.57
GK5	0	20.14	32.38	46.14	55.12	66.24	70.45	76.14	79.21	85.12	81.45	78.54	74.54	71.21
pH 5.6 (Phosphate buffer)														
GK2	0	8.47	16.12	20.15	26.14	30.12	36.14	42.14	54.12	63.12	58.14	53.01	49.21	46.12
GK5	0	15.14	28.21	40.57	46.21	53.45	58.65	62.98	68.45	72.24	68.21	62.14	58.36	55.12

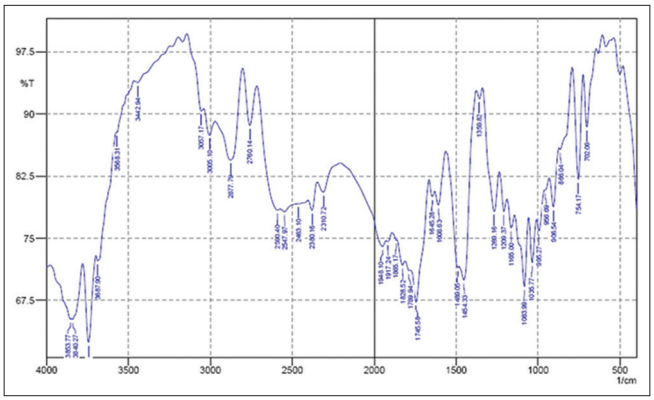

Figure 11: Fourier transform infrared spectra of ketoconazole+physical mixture of polymers

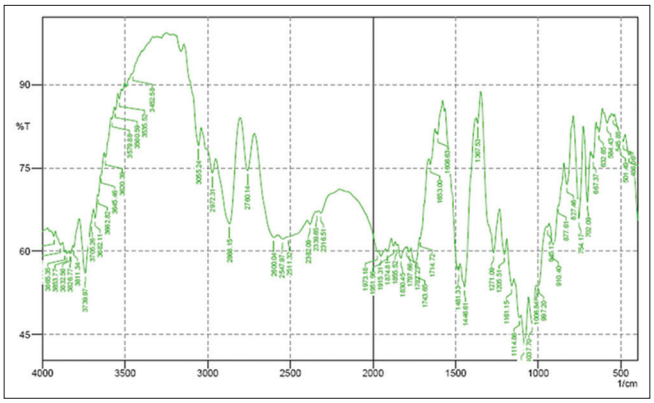

Figure 12: Fourier transform infrared spectra of ketoconazole nanosponges

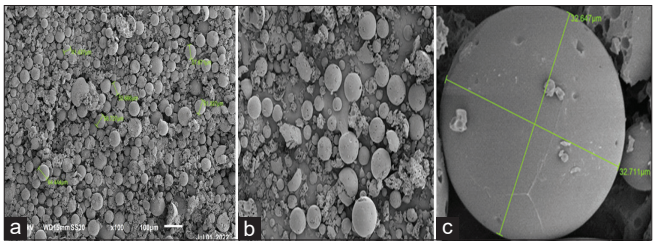

Figure 13: Particle size analysis (a: ×100, b: ×500, and c: ×1000, 32.711 µm and 43 µm, 56.76 µm)

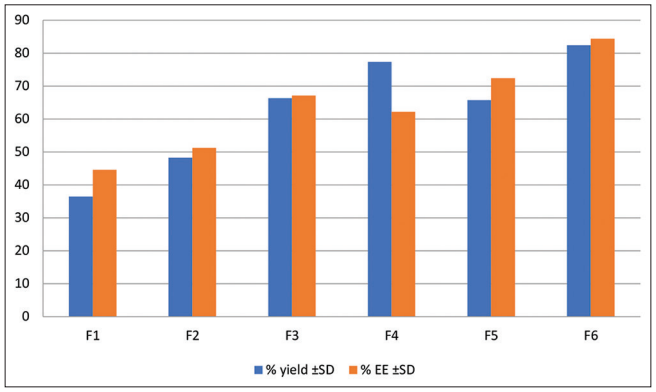

Figure 14: Comparative % yield and % entrapment efficiency for F1-F6 ketoconazole nanosponges

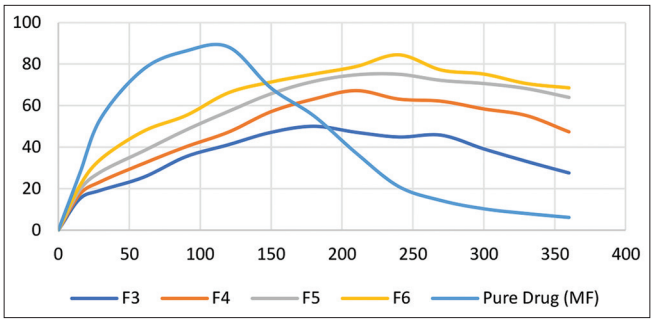

Figure 15: Comparative % *in vitro* drug release: Ketoconazole-nanosponges (F3-F6) and pure drug at PO_4 buffer (pH 6.8)

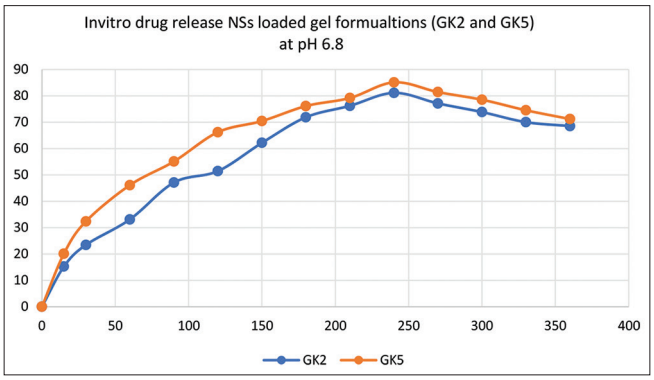

Figure 16: Schematic representation of drug release: Nanosponge-loaded gels (GK2 and GK5 formulations) at pH 6.8 (phosphate buffer)

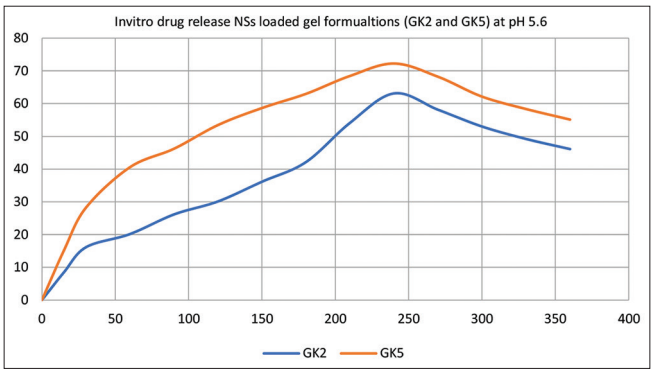

Figure 17: Schematic representation of drug release: Nanosponge-loaded gels (GK2 and GK5 formulations) at pH 5.6 (phosphate buffer)

Table 15: Antifungal activity and ZOI of *Candida albicans* species for various formulation samples

Codes	ZOI (mm)±SD
N (negative control)	00
C (pure drug)	30±0.11
D (drug-loaded nanosponges)	34±0.21
M (marketed formulations of nanosponges)	29±0.14
G (NSs-loaded gel)	33±0.16
T (marketed formulation gel)	32±0.18

*SD: Standard deviation, *n*=3

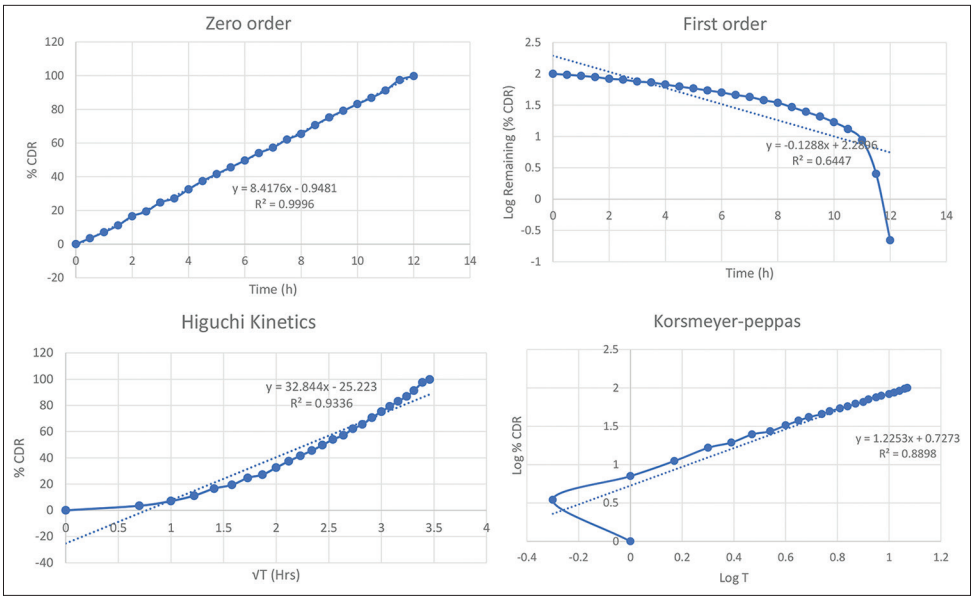

Figure 18: Graphs of drug release kinetic modeling of optimized formulation (GK5)

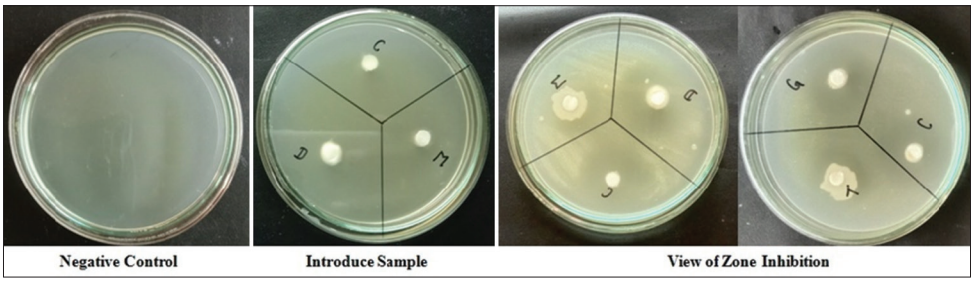

Figure 19: Zone of inhibitions against *Candida albicans*

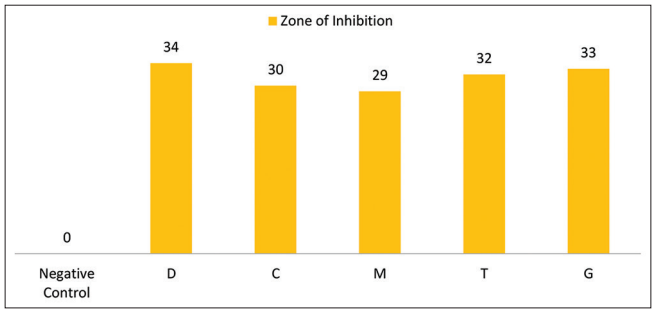

Figure 20: Schematic representation of zone of inhibitions for antifungal activity against *Candida albicans* for various formulation samples

to the free diffusion of the drug into culture media, as shown in Figures 18-20, Table 15. The results suggested that the prepared microspheres-loaded gels were considered to have promising antifungal effects.

CONCLUSIONS

KET-loaded EC NSs were formulated using the solvent evaporation method for topical delivery and a controlled release mechanism to reduce the side effects of conventional medication. Varying drug: polymer ratios, drug content, drug EE, and % yield showed remarkable effects. Formulation F6 was selected for further studies based on excellent and satisfactory results among the prepared KET-loaded NSs (KET-NSs). The F6 formulation showed superior % drug content, % yield, and EE, showing extended drug release of drug (84.48) at the end of 240 min. This suggested that sustained effect was observed, and prepared formulations were targeted to reduce side effects of conventional medication such as irritation and hypersensitivity. Optimized F6 formulation was loaded into gel bases HPMC and carbopol-934. The results suggested that the optimized formulation of KET-NSs-loaded HPMC gel (GK5) showed better results, effectively targeted fungal infection, and provided potent applications for cosmeceuticals and topical delivery. The (r^2) values for diffusion profiles of optimized KET-based HPMC gel (GK5) followed zero-order kinetics and n value (1.2253), suggesting that the release mechanism is a non-Fickian diffusion model. Formulations GK5 showed more residence time at the site of application and provided controlled and prolonged drug release over 12 h.

ACKNOWLEDGMENTS

All contributed equally to this paper.

Limitations

- Only one strain was selected for the study
- The study requires further findings of *in vivo* activity for a better conclusion.

Rationale of current research

- Nanosponges are nanoparticles having tiny interconnected voids, capable of entrapping both lipophilic and hydrophilic drug molecules
- They are explored for multifaced properties such as target drug delivery, improving aqueous solubility, improving bioavailability, and residence time at the target site
- Nanosponge-based gels of antifungal agents are prepared to improve residence time, penetration into deeper skin tissues, and avoid conventional medication side effects.

REFERENCES

1. Pawar K, Gadhave R, Waydande S, Pawar P. Recent trends in antifungal agents: A reference to formulation, characterization and applications. Drug Deliv Lett 2019;9:199-210.
2. Available from: https://www.msdmanuals.com/en-in/home/skin-disorders/fungal-skin-infections/overview-of-fungal-skin-infections [Last accessed on 2023 Dec 10].
3. Singh A, Bhatt NA, Goswami A, Kumar A, Sinha A. Role of treatment of amphotericin-B in black fungus treatment: A review article. Ann Rom Soc Cell Biol 2021;25:447-55.
4. Venugopal J, Prabhakaran MP, Low S, Choon AT, Zhang YZ, Deepika G, *et al*. Nanotechnology for nanomedicine and delivery of drugs. Curr Pharm Des 2008;14:2184-200.
5. Nasir A. Nanotechnology and dermatology: Part II--risks of nanotechnology. Clin Dermatol 2010;28:581-8.
6. Guterres SS, Alves MP, Pohlmann AR. Polymeric nanoparticles, nanospheres and nanocapsules, for cutaneous applications. Drug Target Insights 2007;2:147-57.
7. B Archana B, Vaishnavi B, Sindhu K, Goud KM, Sai poojitha D. Formulations and evaluations of repaglinide microspheres by ionotropic gelation technique. Int J Exp Biomed Res 2025;41:1-8.
8. Ahmed RZ, Patil G, Zaheer Z. Nanosponge - a completely new nano-horizon: Pharmaceutical applications and recent advances. Drug Dev Ind Pharm 2013;39:1263-72.
9. Sriniwas, P, Sreeja, K. Formulation and evaluation of voriconazole loaded nanosponges for oral and topical delivery. Int J Drug Dev Res 2013;5:55-69.
10. Martín MJ, Calpena AC, Fernández F, Mallandrich M, Gálvez P, Clares B. Development of alginate microspheres as nystatin carriers for oral mucosa drug delivery. Carbohydr Polym 2015;117:140-9.
11. Pandey, J, Amandeep S. Formulation and evaluation of nanosponge based controlled release topical gel preparation of ketoconazole. Int J Pharm Pharm Res 2018;12:367-82.
12. Available from: https://pubchem.ncbi.nlm.nih.gov/compound/ketoconazole#section=names-and-identifiers [Last accessed on 2024 Dec 26].
13. Available from: https://www.msdmanuals.com/en-in/home/skin-disorders/fungal-skin infections/overview-of-fungal-skin-infections [Last accessed on 2024 Dec 26].
14. Available from: https://www.msdmanuals.com/en-in/home/skin-disorders/fungal-skin-infections/candidiasis-yeast-infection [Last accessed on 2024 Dec 26].
15. Available from: https://www.msdmanuals.com/en-in/home/skin-disorders/fungal-skin-infections/dermatophytid-reaction [Last accessed on 2024 Dec 26].
16. Available from: https://www.msdmanuals.com/en-in/home/skin-disorders/fungal-skin-infections/intertrigo [Last accessed on 2024 Dec 26].
17. Available from: https://www.msdmanuals.com/en-in/home/skin-disorders/fungal-skin-infections/athletes-foot-tinea-pedis [Last accessed on 2024 Dec 26].
18. Available from: https://www.msdmanuals.com/en-in/home/skin-disorders/fungal-skin-infections/jock-itch-tinea-cruris [Last accessed on 2024 Dec 26].
19. Gupta M, Chandra A, Aggarwal G. Curcumin: Potential therapeutic moiety for fungal infections. Curr Tradit Med 2018;4:249-62.
20. Vergidis P. Available from: https://www.merckmanuals.com/professional/infectious- diseases/fungi/aspergillosis [Last accessed on 2024 Dec 28].
21. Brown GD, Ballou ER, Bates S, Bignell EM, Borman AM, Brand AC, *et al*. The pathobiology of human fungal infections. Nat Rev Microbiol 2024;22:687-704.
22. Revie NM, Iyer KR, Robbins N, Cowen LE. Antifungal drug resistance: Evolution, mechanisms and impact. Curr Opin Microbiol 2018;45:70-6.
23. Kaur M, Nagpal M, Singh M, Singh TG, Aggarwal G, Dhingra GA. Improved antibacterial activity of topical gel-based on nanosponge carrier of cinnamon oil. Bioimpacts 2021;11:23-31.
24. Kumar S, Pooja, Trotta F, Rao R. Encapsulation of babchi oil in cyclodextrin-based nanosponges: Physicochemical characterization, photodegradation, and *in vitro* cytotoxicity studies. Pharmaceutics 2018;10:169.
25. Song SH, Lee KM, Kang JB, Lee SG, Kang MJ, Choi YW. Improved skin delivery of voriconazole with a nanostructured lipid carrier-based hydrogel formulation. Chem Pharm Bull (Tokyo) 2014;62:793-8.
26. Popovska O, Kavrakovski Z, Rafajlovska V. Development and validation of UV spectroscopic method for determination of ketoconazole in pharmaceutical formulations. Int J Pharm 2014;4:95-101.
27. Balu M, Subudhi SK, Zubair S, Navya S, Naaz R,

Mounika S. Development and validation of ketoconazole by RP-HPLC. Int J Adv Res Med Pharm Sci 2019;4:1-8.
28. Sodeifian G, Sajadian SA, Razmimanesh F, Hazaveie SM. Solubility of ketoconazole (antifungal drug) in SC-CO_2 for binary and ternary systems: Measurements and empirical correlations. Sci Rep 2021;11:7546.
29. Cumming H, Rücker C. Octanol-water partition coefficient measurement by a simple ^{1}HNMR. ACS Omega 2017;2:6244-9.
30. Kumar S, Prasad M, Rao R. Topical delivery of clobetasol propionate loaded nanosponge hydrogel for effective treatment of psoriasis: Formulation, physicochemical characterization, antipsoriatic potential and biochemical estimation. Mater Sci Eng C Mater Biol Appl 2021;119:111605.
31. Ghose A, Nabi B, Rehman S, Shadab M, Alhakamy NA, Ahmad OA, *et al*. Development and evaluation of polymeric nanosponge hydrogel for terbinafine hydrochloride: Statistical optimization, *in vitro* and *in vivo* studies. Polymers (Basel) 2020;12:2903.
32. Kadian V, Rao R. Enhancing anti-inflammatory effect of brucine nanohydrogel using rosemary oil: A promising strategy for dermal delivery in arthritic inflammation. 3 Biotech 2024;14:157.
33. Sivadasan D, Venkatesan K, Mohamed JM, Alqahtani S, Asiri YI, Faisal MM, *et al*. Application of 3^2factorial design for loratadine-loaded nanosponge in topical gel formulation: Comprehensive *in-vitro* and *ex vivo* evaluations. Sci Rep 2024;14:6361.
34. Shen C, Shen B, Zhu J, Yuan H, Hu J. Topical delivery of pluronic F127/TPGS mixed micelles-based hydrogel loaded with glycyrrhizic acid for atopic dermatitis treatment. Drug Dev Ind Pharm 2021;47:1975-85.
35. Stolić Jovanović A, Martinović M, Žugić A, Nešić I, Tosti T, Blagojević S, *et al*. Derivatives of L-ascorbic acid in emulgel: Development and comprehensive evaluation of the topical delivery system. Pharmaceutics 2023;15:813.
36. Pavic A, Stojanovic Z, Pekmezovic M, Veljović Đ, O'Connor K, Malagurski I, *et al*. Polyenes in medium chain length polyhydroxyalkanoate (mcl-PHA) biopolymer microspheres with reduced toxicity and improved therapeutic effect against *Candida* infection in zebrafish model. Pharmaceutics 2022;14:696.
37. Jovanovic AS, Martinovic M, Zugic A, Nesic I, Tosti T, Blagojevic S, Tadic VM. Derivatives of L-ascorbic acid in emulgel: Development and comprehensive evaluation of the topical delivery system. Pharmaceutics 2023;15:813.
38. Nanda S, Saroha K, Sharma B. Formulation, evaluation and optimization of transdermal gel of ketorolac tromethamine using face centered central composite design. Int J Pharm Pharm Sci 2014;6:133-9.
39. Kaur LP, Garg R, Gupta GD. Development and evaluation of topical gel of minoxidil from different polymer bases in application of alopecia. Int J Pharm Pharm Sci 2010;2:43-7.
40. Basha NB, Prakasam K, Goli D. Formulation and evaluation of gel containing fluconazole-antifungal agent. Int J Drug Dev Res 2011;3:109-28.
41. Sera UV, Ramana MV. *In vitro* skin absorption and drug release - A comparison of four commercial hydrophilic gel preparations for topical use. Indian Pharm 2006;73:356-60.
42. Marchiori MC, Rigon C, da S Jardim F, Giuliani LM, Copetti PM, Sagrillo MR, *et al*. Hydrogel containing silibinin-loaded pomegranate oil-based nanocapsules for cutaneous application: *In vitro* safety investigation and human skin biometry and permeation studies. AAPS PharmSciTech 2023;24:138.
43. Shen M, Zheng L, Koole LH. Polymeric microspheres designed to carry crystalline drugs at their surface or inside cavities and dimples. Pharmaceutics 2023;15:2146.
44. Hariyadi DM, Fitri A, Sudarma S, Purwanti T, Erawati T. Optimization of microspheres containing virgin coconut oil and hydrolyzed virgin coconut oil as antimicrobial. J Adv Pharm Technol Res 2022;13:238-42.
45. Chen X, Jiang Z, Lin Y, Yu C, Nie X, Xu G, *et al*. Tumor lysates-constructed hydrogel to potentiate tumor immunotherapy. J Control Release 2023;358:345-57.
46. Farooq M, Ihsan J, Mohamed RM, Khan MA, Rehman TU, Ullah H, *et al*. Highly biocompatible formulations based on Arabic gum nano composite hydrogels: Fabrication, characterization, and biological investigation. Int J Biol Macromol 2022;209:59-69.
47. Alsakhawy SA, Baghdadi HH, El-Shenawy MA, Sabra SA, El-Hosseiny LS. Encapsulation of *Thymus vulgaris* essential oil in caseinate/gelatin nanocomposite hydrogel: *In vitro* antibacterial activity and *in vivo* wound healing potential. Int J Pharm 2022;628:122280.
48. Li H, Liang X, Sun W, Zhuang B, Cao Y, Zhang J, *et al*. Immunological evaluation of a recombinant vaccine delivered with an analogous hyaluronic acid chitosan nanoparticle-hydrogel against *Toxoplasma gondii* in mice. Microb Pathog 2023;179:106092.
49. Mohsen AM, Nagy YI, Shehabeldine AM, Okba MM. Thymol-loaded eudragit RS30D cationic nanoparticles-based hydrogels for topical application in wounds: *In vitro* and *in vivo* evaluation. Pharmaceutics 2022;15:19.
50. Jahromi LP, Rothammer M, Fuhrmann G. Polysaccharide hydrogel platforms as suitable carriers of liposomes and extracellular vesicles for dermal applications. Adv Drug Deliv Rev 2023;200:115028.
51. Rehman S, Madni A, Jameel QA, Usman F, Raza MR, Ahmad F, *et al*. Natural polymer-based graphene oxide bio-nanocomposite hydrogel beads: Superstructures with advanced potentials for drug delivery. AAPS PharmSciTech 2022;23:304.
52. Zahra D, Shokat Z, Ahmad A, Javaid A, Khurshid M, Ashfaq UA, *et al*. Exploring the recent developments of alginate silk fibroin material for hydrogel wound dressing:

A review. Int J Biol Macromol 2023;248:125989.
53. Moreno Ruiz YP, de Almeida Campos LA, Alves Agreles MA, Galembeck A, Macário Ferro Cavalcanti I. Advanced hydrogels combined with silver and gold nanoparticles against antimicrobial resistance. Antibiotics (Basel) 2023;12:104.
54. Ryan A, Patel P, Ratrey P, O'Connor PM, O'Sullivan J, Ross RP, *et al*. The development of a Solid Lipid Nanoparticle (SLN)-based lacticin 3147 hydrogel for the treatment of wound infections. Drug Deliv Transl Res 2023;13:2407-23.
55. Sha X, Chan L, Fan X, Guo P, Chen T, Liu L, *et al*. Thermosensitive tri-block polymer nanoparticle-hydrogel composites as payloads of natamycin for antifungal therapy against *Fusarium solani*. Int J Nanomedicine 2022;17:1463-78.

Source of Support: Nil. **Conflicts of Interest:** None declared.